Applications of generalized integral transform technique in the rapid solidification of metallic metals in the planar flow casting process

Aplicações da técnica de transformação integral generalizada na solidificação rápida de metais metálicos no processo de fundição em fluxo planar

DOI:10.34117/bjdv8n4-208

Recebimento dos originais: 21/02/2022
Aceitação para publicação: 31/03/2022

Marinaldo José de Medeiros
Doutorando em Engenharia Mecânica pela UFPB/PPGEM
Institution: IFPB Campus Itabaiana
Address: Via Expressa Padre Zé, s/n - Cidade Universitária, CEP: 58051-970 - João Pessoa/PB Brasil
E-mail: marinaldo.medeiros@ifpb.edu.br

Mabel de Morais Lopes
Doutora em Engenharia Mecânica pela UFPB/PPGEM
Institution: UFPB/PPGEM
Address: Via Expressa Padre Zé, s/n - Cidade Universitária, CEP: 58051-970 - João Pessoa/PB – Brasil
E-mail: mabel.m.lopes@gmail.com

Thiago da Silva André
Doutorando em Engenharia Mecânica pela UFPB/PPGEM
Institution: UFPB/PPGEM
Address: Via Expressa Padre Zé, s/n - Cidade Universitária, CEP:58051-970 - João Pessoa/PB – Brasil
E-mail: andre.thiago@ifrn.edu.br

Ariel Aires do Nascimento
Doutor em Engenharia Mecânica pela IFPB Campus João Pessoa
Institution: IFPB Campus João Pessoa
Address: Avenida Primeiro de Maio, 720 - Jaguaribe, CEP:58.015-435– João Pessoa/ PB – Brasil
E-mail: ariel@ifpb.edu.br

Jesus Marlinaldo de Medeiros
Doutor em Engenharia Mecânica pela IFPB Campus Cabedelo
Institution: IFPB Campus Cabedelo
Address: Rua Santa Rita de Cássia, 1900, Jardim Camboinha, Cabedelo – PB, CEP: 58103-772
E-mail: jesus.medeiros@ifpb.edu.br

Carlos Antonio Cabral dos Santos
Doutor em Engenharia Mecânica pela UFPB/CT
Institution: UFPB/CT
Address: Via Expressa Padre Zé, s/n - Cidade Universitária, CEP:58.051-900– João Pessoa/ PB – Brasil
E-mail: carloscabralsantos@yahoo.com.br

ABSTRACT
The Planar Flow Casting (PFC) is a single-stage fast solidification technique to produce thin metallic ribbons. The objective of this research is to develop a mathematical model to analyze the phenomenon of heat transfer and phase change during the formation of the puddle, to determine the interface position and velocity and the temperature profile. The applied methodology consists of the use of the energy balance, where the equations of the energy (liquid and solid phases), and the equation of the interface are transformed through the Generalized Integral Transform Technique (GITT) being solved by the NDSolve routine of the Matemathica. This tool was capable to solve problem, can study the fast cooling of metals and obtain ribbons of thickness controlled by the speed of the wheel and for the heat transfer coefficient. Considering that the height of the pool is very small and the process time is very short, many eigenvalues were used to obtain the solution convergence. The results of the temperature distribution along the length of the puddle, the evolution of the solidification front and the interface velocity were compared with existing results in the literature, obtaining good harmony.

Keywords: moving boundary, planar flow casting, generalized integral transform technique.

RESUMO
O Processo de fundição em fluxo planar (Planar Flow Casting) é uma técnica de solidificação rápida de estágio único para produção de fitas metálicas finas. O objetivo desta pesquisa é desenvolver um modelo matemático para analisar o fenômeno de transferência de calor e mudança de fase durante a formação da poça, para determinar a posição e a velocidade da interface e o perfil de temperatura. A metodologia aplicada consiste na utilização do balanço de energia, onde as equações da energia (fases líquida e sólida), e a equação da interface são transformadas através da Técnica da Transformada Integral Generalizada (GITT) sendo resolvidas pela rotina NDSolve do Matemathica. Esta ferramenta foi capaz de resolver o problema, pode estudar o resfriamento rápido de metais e obter fitas de espessura controlada pela velocidade da roda e pelo coeficiente de transferência de calor. Considerando que a altura da poça é muito pequena e o tempo de processo muito curto, muitos autovalores foram utilizados para obter a convergência da solução. Os resultados da distribuição de temperatura ao longo do comprimento da poça, da evolução da frente de solidificação e da velocidade da interface foram comparados com resultados existentes na literatura, obtendo-se boa harmonia.

Palavras chave: fronteira móvel, processo de fluxo planar, técnica da transformada integral generalizada.

1 INTRODUCTION

Transient phase change problems involve the path followed by a movement of the solidification front, separating the liquid and solid phases of a substance. Inside of the liquid phase and the solid phase the process of transfer of heat is governed mainly by conduction. The Planar Flow Casting (PFC) is a complicated solidification process, where heat and mass transfer, multiphase fluid flow and solidification occur concurrently. During the PFC process, molten alloy is continuously deposited into a substrate of a cooling wheel through a nozzle slot. Upon contacting the substrate of cooling wheel, the molten alloy rapidly solidified and continuous ribbon is peeled off from the wheel and coiled by a winding machine.

The temper starting from the liquid metal is a process of rapid solidification that involves the shock with spreading and appearance of the solidification starting from the puddle of liquid metal on the surface of a substrate. Contrary to the traditional process of production, where the temper is made on sample of solid material, the rapid cooling starting from the liquid metal represents a separate category from temper in that the initial state of the metal is liquid (JONES, 1984; ANNAVARAPU et al., 1990).

This leads to a characteristic definition of the method of rapid cooling starting with the liquid metal, which is imposed by the speeds of cooling of the liquid metal, that are typically much faster than the conventional methods of temper. This situation happens when the heat transfer mechanism, mainly conduction, can remove much faster the heat that comes out of the deposition layer than the heat that is deposited by the liquid metal. The fluid dynamics of the rapid solidification processes have also been the focus of many studies, the effects of heat transfer and PHASE change in planar flow casting processes was studied numerically by Wang and Matthys (1991, 1992); Carpenter and Steen (1992). Liu et al. (1993) investigated numerically the substrate impact and freezing of molten droplets in plasma spray processes.

Since the 90s, the industry has been showing interest in the technology of fast solidification of metals and alloys starting from the liquid state, because of its compact form and production capacity with fast performance, as well as an improvement of the properties of the materials. Carpenter and Steen (1997) and Steen and Karcher (1997) provide a review of the fluid mechanics of the PFC process. Numerous studies have investigated the influences of casting parameters and casting conditions on the uniformity of ribbon thickness and the surface quality of peeled ribbon (WANG and PRASAD, 2000; WANG and MATTHYS, 2001; NASCIMENTO, 2002; BUSSMANN et al., 2002;

NAPOLITANO and MECO, 2004). Byrne et al. (2006) investigate the capillary puddle vibration on casting defect of ribbons in PFC process. Wang et al. (2010) studied the thermal and mechanical behavior of the solidifying shell during continuous steel casting. Liu et al. (2009a, b, 2010); Cox (2011); Swaroopa et al. (2015); Su et al. (2015, 2016) studied the dependence of ribbon thickness on the main process parameters and to develop a simple formulation that predicts the ribbon thickness in gap-controlled PFC process. (LI et al., 2017; SWAROOPA et al., 2017). Mattson et al. (2018); Mattson (2019) studied crystalline and non-crystalline alloys using the PFC process and it was found that the tape thickness depends on the thermal properties of the alloy and the heat transfer characteristics of the machine used to produce the tape. (MU et al., 2020; LI and LU, 2020; MADIREDDI, 2020; THEISEN and WEINSTEIN, 2021) reviewed how PFC processes were developed, examined the typical operability range of PFC, and reviewed the defects that commonly form. Medeiros and Santos (2021) studied the behavior of interface of the rapid solidification of aluminum in planar flow casting process. Currently, the use of computational simulation tools has grown considerably, combined with the optimization of the production process to modernize the manufacturing process of metallic parts, as well as carrying out experiments, in order to improve the properties of materials through the study of parameters, that reduce or attenuate defects and cracks in the solidification process. (PAZ et al. 2020 and FRANÇA et al. 2020).

The main objective of this article is through mathematical model proposed analyze the phenomenon of heat transfer and phase change to determine the position of the interface, the interface velocity and the temperature field to obtain well-finished metallic tapes or alloys with excellent properties through the application of Generalized Integral Transformation Technique (GITT) varying the heat transfer coefficient and using a constant uniform velocity flywheel already known in the literature, obtaining good results in comparison with the literature.

2 PLANAR FLOW CASTING PROCESS

The Planar Flow Casting (PFC) is a single-stage fast solidification technique to produce thin metallic ribbons where the liquid metal in the crucible is forced through the hole and it forms the solidification puddle between the base of the crucible and the surface of wheel. The ribbon is dragged out of the melt puddle by the relative substrate motion depending on the heat transfer, nucleation and crystal growth characteristics, conform show in Fig. 1

Figure 1. Schematic Diagram of the PFC Geometry used in Model.

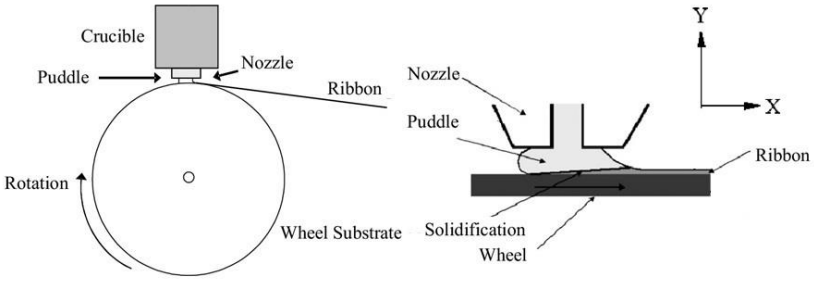

Fonte: Medeiros and Santos [2021]

With the objective of making the model as simple as possible, let us consider that gradient of speed doesn´t exist in the puddle. In fact, this is not true, and it represents an approximation of a real case. To identify relative tendencies and to investigate important parameters in the process, we will adopt a one-dimensional model (WANG and MATTHYS, 1991, 1992), where the main simplifying hypotheses adopted were: Laminar flow; steady state; local thermodynamic equilibrium in the interface solid/liquid and constant specific mass for both phases.

With the assumptions considered above and assuming that a thin, immobile layer of liquid metal is suddenly brought into contact with the cooling substrate, in a very short period, then the liquid metal solidifies. If there is no relative movement between the fluid flow and the wheel, and if the deposited metallic layer (puddle) is thin, and, due to the decoupling between the heat transfer process and the mechanics of the fluid flow, caused by the high speed of the substrate, we can approximate the heat transfer in the deposited metallic layer and in the substrate, with only one-dimensional conduction. Then, the energy equations for the boundary layer in each region are given, such as:

Solid Region:

$$V_w \frac{\partial T_S}{\partial \mathrm{x}} = \alpha_S \frac{\partial^2 T_S}{\partial y^2} \; ; \; 0 < \mathrm{y} < S(t) \; ; \; t > t_0 \qquad (1)$$

Liquid Region:

$$V_w \frac{\partial T_L}{\partial \mathrm{x}} = \alpha_L \frac{\partial^2 T_L}{\partial y^2} \; ; \; S(t) < \mathrm{y} < L; \; t > t_0 \qquad (2)$$

Interface

$$K_S \frac{\partial T_S}{\partial \mathrm{y}} - K_L \frac{\partial T_L}{\partial \mathrm{y}} = \rho \Delta H \frac{\partial S(t)}{\partial \mathrm{t}} \; ; \; \mathrm{y} = S(t) \; ; \; t > t_0 \qquad (3)$$

And boundary conditions:

$$K_S \frac{\partial T_S}{\partial y} = h_w\,(T_S - T_\infty)\ \ ;\ y = 0\ ;\ t > t_0 \tag{4}$$

$$T_S = T_L = T_m\ \ ;\ y = S(t)\ ;\ t > t_0 \tag{5}$$

$$T_L = T_0\ \ ;\ y = 0\ ;\ t > t_0 \tag{6}$$

Where $T_{S\ e\ L}$, $\alpha_{S\ e\ L}$ are, respectively, the temperatures, the thermal diffusivity and the thermal conductivities of the solid and liquid phases. V_w is the speed of the wheel, h_w the heat transfer coefficient, T_∞ is the temperature of the atmosphere and wheel, T_m the temperature of phase change, T_0 the intial temperature of the metal, ρ is the specific mass of the metal, ΔH is latent heat of phase change of the metal and S(t) is the front position of solidification in the direction y.

Because of the supposition that relative movement does not exit inside of the liquid metal in the puddle, the two-dimensional problem for the limit layer in permanent state can be reduced to a one-dimensional heat conduction problem. For that we will make $x=V_f\ t$, where V_f is the medium speed of the metal on the wheel. Considering that the drainage in the puddle is completely developed, so that the speed of the wheel V_w is the same as the medium speed of the metal on the wheel V_f, substituting $x= V_f\ t$ in the solid and liquid region equations can also be rewritten after introducing the following dimensionless groups:

$$\eta_1 = \frac{y}{S(t)}\ \ ;\ \ \eta_2 = \frac{y-L}{S(t)-L}\ \ ;\ \ Bi = \frac{h_w\,L}{K_S}\ \ ;\ \ \nu = \sqrt{\frac{\alpha_L}{\alpha_S}}\ \ ;\ \ S(\tau) = \frac{S(t)}{L} \tag{7}$$

$$\tau = \frac{\alpha_L\,t}{L^2}\ \ ;\ \theta_S = \frac{T_S - T_\infty}{T_m - T_\infty}\ \ ;\ \theta_L = \frac{T_L - T_\infty}{T_m - T_\infty}\ \ ;\ Ste_L = \frac{CP_L(T_m - T_0)}{\Delta H}\ ;\ Ste_S = \frac{CP_S(T_m - T_\infty)}{\Delta H} \tag{8}$$

And introduce a domain regularization for the spatial domain written:

$$\frac{\partial}{\partial y} = \frac{\partial}{\partial \eta_i}\frac{\partial \eta_i}{\partial y}\ \ ;\ \frac{\partial}{\partial t} = \frac{\partial}{\partial \tau}\frac{\partial \tau}{\partial t} + \frac{\partial}{\partial \eta_i}\frac{\partial \eta_i}{\partial \tau}\ \ for\ i = 1(solid)\ and\ \ i = 2\ (liquid) \tag{9}$$

Then, the dimensionless form for solid and liquid region and interface equations after the domain transformation for the spatial domain written as:

Solid Region:

$$\frac{\partial \theta_S}{\partial \tau} = \frac{1}{\nu^2 S(\tau)^2}\frac{\partial^2 \theta_S}{\partial \eta_1^2} + \eta_1 \frac{S'(\tau)}{S(\tau)}\frac{\partial \theta_S}{\partial \eta_1}\ ;\ 0 < \eta_1 < 1\ ;\ \tau > \tau_0 \tag{10}$$

Liquid Region:

$$\frac{\partial \theta_L}{\partial \tau} = \frac{1}{(S(\tau)-1)^2}\frac{\partial^2 \theta_L}{\partial \eta_2^2} + \eta_2 \frac{S'(\tau)}{(S(\tau)-1)}\frac{\partial \theta_S}{\partial \eta_2}\ ;\ 0 < \eta_2 < 1\ ;\ \tau > \tau_0 \quad (11)$$

Interface

$$\frac{dS(\tau)}{d\tau} = \frac{Ste_S}{\nu^2 S(\tau)}\frac{\partial \theta_S}{\partial \eta_1}\Big|_{\eta_1=1} - \frac{Ste_L}{(S(\tau)-1)}\frac{\partial \theta_L}{\partial \eta_2}\Big|_{\eta_2=1} \quad (12)$$

And boundary conditions:

$$-\frac{\partial \theta_S(0,\tau)}{\partial \eta_1} + Bi\, S(\tau)\theta_S(0,\tau) = 0\ ;\ \ \tau > \tau_0 \quad (13)$$

$$\theta_S(1,\tau) = 1\ ;\ \theta_L(1,\tau) = 1\ ;\ \tau > \tau_0 \quad (14)$$

$$\theta_L(0,\tau) = 0\ ;\ \tau > \tau_0 \quad (15)$$

3 METHODOLOGY

With the objective of improving the performance of GITT, it is necessary to homogenize the boundary conditions of problem

$$\theta_S(\eta_1,\tau) = F_S(\eta_1;\tau) + \phi_S(\eta_1,\tau)\ ;\ \theta_L(\eta_2,\tau) = F_L(\eta_2;\tau) + \phi_L(\eta_2,\tau) \quad (16)$$

The solutions to the filter equations are given by:

$$F_S(\eta_1;\tau) = \frac{Bi\, S(\tau)\eta_1 + 1}{1 + Bi\, S(\tau)} = f(\tau)\ ;\quad F_L(\eta_2;\tau) = \eta_2 \quad (17)$$

Inserting the filters in the solid and liquid region and interface equations, we obtain:

$$\frac{\partial \phi_S}{\partial \tau} = \frac{1}{\nu^2 S(\tau)^2}\frac{\partial^2 \phi_S}{\partial \eta_1^2} + \eta_1 \frac{S'(\tau)}{S(\tau)}\left(\frac{\partial \phi_S}{\partial \eta_1} + f(\tau)\right) - f'(\tau)\ ;\ 0 < \eta_1 < 1\ ;\ \tau > \tau_0 \quad (18)$$

$$\frac{\partial \phi_L}{\partial \tau} = \frac{1}{(S(\tau)-1)^2}\frac{\partial^2 \phi_L}{\partial \eta_2^2} + \eta_2 \frac{S'(\tau)}{(S(\tau)-1)}\left(\frac{\partial \phi_S}{\partial \eta_2} + 1\right)\ ;\ 0 < \eta_2 < 1\ ;\ \tau > \tau_0 \quad (19)$$

$$\frac{dS(\tau)}{d\tau} = \frac{Ste_S}{\nu^2 S(\tau)}\left(\frac{\partial \theta_S}{\partial \eta_1} + \frac{Bi\, S(\tau)}{1 + Bi\, S(\tau)}\right)\Big|_{\eta_1=1} - \frac{Ste_L}{(S(\tau)-1)}\left(\frac{\partial \theta_L}{\partial \eta_2} + 1\right)\Big|_{\eta_2=1} \quad (20)$$

Following the basic steps of GITT (ÖZISIK (1993), MIYAGAWA et al. (2019) and COTTA (2020)), the appropriate auxiliary problems for the process of integral transform, are given as follows:

Solid Region

$$\frac{d^2\psi_i(\eta_1)}{d{\eta_1}^2} + \mu_i^2\psi_i(\eta_1) = 0 \ ; \ -\frac{d\psi_i(0)}{d\eta_1} + Bi\ S(\tau)\psi_i(0) = 0 \ ; \ \psi_i(1) = 0, \quad (21)$$

Which is readily solved eigenfunctions, normalized eigenfunctions, eigenvalues and norms, respectively, as:

$$\psi_i(\eta_1) = Sin[\mu_i(1-\eta_1)] \ ; \ \widetilde{\psi_i}(\eta_1) = \frac{\psi_i(\eta_1)}{\sqrt{N_i}} \ ; \ \mu_i Cos[\mu_i] = Bi\ S(\tau) Sin[\mu_i] \quad (22)$$

$$N_i = \int_0^1 \psi_i(\eta_1)^2\, d\eta_1 = \frac{(Bi\ S(\tau))^2 + Bi\ S(\tau) + \mu_i^2}{2\left(\left(Bi\ S(\tau)\right)^2 + \mu_i^2\right)} \quad (23)$$

Liquid Region

$$\frac{d^2\chi_i(\eta_2)}{d{\eta_2}^2} + \xi_i^2\chi_i(\eta_2) = 0 \ ; \ \chi_i(0) = 0 \ ; \ \chi_i(1) = 0, \quad (24)$$

Which is readily solved eigenfunctions, normalized eigenfunctions, eigenvalues and norms, respectively, as:

$$\chi_i(\eta_2) = Sin[\xi_i\eta_2] \ ; \ \widetilde{\chi_i}(\eta_2) = \frac{\chi_i(\eta_2)}{\sqrt{M_i}} \ ; \ \xi_i = i\,\pi \quad (25)$$

$$M_i = \int_0^1 \chi_i(\eta_2)^2\, d\eta_2 = \frac{1}{2} \quad (26)$$

The eigenvalue problems Eqs. (21) and (24) allows definition of the following transform-inverse pairs:

$$\overline{\phi_{S_J}}(\tau) = \int_0^1 \widetilde{\psi_J}(\eta_1)\, \phi_S(\eta_1, \tau) d\eta_1 \ \rightarrow Transform \quad (27)$$

$$\phi_S(\eta_1, \tau) = \sum_{j=1}^{\infty} \widetilde{\psi_J}(\eta_1)\overline{\phi_{S_J}}(\tau) \quad \rightarrow Inverse \quad (28)$$

$$\overline{\phi_{L_J}}(\tau) = \int_0^1 \widetilde{\chi_J}(\eta_2)\, \phi_L(\eta_2, \tau) d\eta_2 \ \rightarrow Transform \quad (29)$$

$$\phi_L(\eta_2, \tau) = \sum_{j=1}^{\infty} \widetilde{\chi_J}(\eta_2)\overline{\phi_{L_J}}(\tau) \quad \rightarrow Inverse \quad (30)$$

Applying the operators over Eq. (17) and (19), followed by the inverse formula then results:

$$\frac{d\overline{\phi_{S_i}}(\tau)}{d\tau} = -\frac{\mu_i^2\overline{\phi_{S_i}}(\tau)}{\nu^2 S(\tau)^2} + \frac{S'(\tau)}{S(\tau)}\sum_{j=1}^{\infty} A_{ij}\overline{\phi_{S_j}}(\tau) + \frac{S'(\tau)}{S(\tau)}\,B_i - \frac{Bi\,S'(\tau)}{\left(1+BiS(\tau)\right)^2}\,g_i \tag{31}$$

$$\frac{d\overline{\phi_{L_i}}(\tau)}{d\tau} = -\frac{\xi_i^2\overline{\phi_{L_i}}(\tau)}{(S(\tau)-1)^2} + \frac{S'(\tau)}{(S(\tau)-1)}\sum_{j=1}^{\infty} C_{ij}\overline{\phi_{L_j}}(\tau) + \frac{S'(\tau)}{(S(\tau)-1)}\,D_i \tag{32}$$

$$\frac{dS(\tau)}{d\tau} = \frac{Ste_S}{\nu^2 S(\tau)}\left[\sum_{j=1}^{\infty}\frac{d\psi_j(1)}{d\eta_1}\overline{\phi_{S_j}}(\tau) + \frac{Bi\,S(\tau)}{1+Bi\,S(\tau)}\right] - \left[\sum_{j=1}^{\infty}\frac{d\chi_j(1)}{d\eta_2}\overline{\phi_{L_j}}(\tau) + 1\right] \tag{33}$$

With

$$A_{ij} = \int_0^1 \eta_1\tilde{\psi}_i(\eta_1)\frac{d\tilde{\psi}_j(\eta_1)}{d\eta_1}d\eta_1 \tag{34}$$

$$B_i = \int_0^1 \eta_1\tilde{\psi}_i(\eta_1)\,d\eta_1 \tag{35}$$

$$C_{ij} = \int_0^1 \eta_2\tilde{\chi}_i(\eta_2)\frac{d\tilde{\chi}_i(\eta_2)}{d\eta_2}d\eta_2 \tag{36}$$

$$D_i = \int_0^1 \eta_2\tilde{\chi}_i(\eta_2)\,d\eta_2 \tag{37}$$

$$g_i = \int_0^1 \tilde{\psi}_i(\eta_1)(1-\eta_1)\,d\eta_1 \tag{38}$$

The initial conditions of the solid and liquid phases temperature field are transformed and written as:

$$\overline{\phi_{S_j}}(\tau_0) = \int_0^1 \widetilde{\psi_j}(\eta_1)\,(\phi_{S_{Analit}}(\eta_1,\tau_0) - F_S(\eta_1,\tau_0))d\eta_1 \tag{39}$$

$$\overline{\phi_{L_j}}(\tau_0) = \int_0^1 \widetilde{\chi_j}(\eta_2)\,(\phi_{L_{Analit}}(\eta_2,\tau_0) - F_L(\eta_2,\tau_0))d\eta_2 \tag{40}$$

Eqs. (31), (32) and (33) form an infinite system of one-dimensional partial differential equations for the transformed potentials. For computational purposes this system is truncated to a sufficient large finite order, NS and NL (liquid and solid region eigenvalues number), for the required converged control. Once the transformed potentials

are numerically computed, the inversion formula, Eqs. (28) and (30), is employed to reconstruct the filtered potentials, in explicit form in the transverse coordinate, and after adding the filtering solution, the dimensionless temperature distribution, is recovered everywhere within the region along the process.

4 RESULTS AND DISCUSSION

The simulation of the planar flow casting process provides the control and adjustment of the parameters involved in the production of metallic ribbons. The relation of those parameters with the heat transfer coefficients makes possible the adjustment of the process and use of different materials. The main parameters involved are ejection temperature, distance from the crucible to the cooling substrate, substrate temperature, substrate speed, height and length of the puddle. For the conduct of the simulations, pure aluminum will be used, whose parameters involved in the solidification processes, have important influences in the monitoring of real and design processes.

To compare the results, we extracted the properties obtained by Wang and Matthys (1992):

$$\Delta H = 3.95\ 10^5 \frac{J}{kg}\ ;\ CP_L = 1200 \frac{J}{kg\ K}\ ;\ CP_S = 1060 \frac{J}{kg\ K}\ ;\ V_w = 23 \frac{m}{s}\ ;$$
$$XD = 5.75mm\ ;\ K_S = 200 \frac{W}{m\ K}\ ;\ K_L = 100 \frac{W}{m\ K}\ ;\ \rho = 2520 \frac{kg}{m^3}$$
$$T_0 - T_m = 50\ K\ ;\ T_\infty = 300K$$

Figure 2 shows the behavior of the temperature curves as a function of the distance to the upper meniscus, where solidification begins, for the aluminum metal on the copper flywheel. At the end of the process, the tape reached a thickness of 114 μm, the temperature is above the solidification temperature, that is, at this thickness everything is liquid. As it moves in the vertical position (y) there is a phase change, in thickness 4 μm there is only solid, the position closer to the copper wheel. You can also see that as you move in the horizontal position (x), the temperature drops considerably, especially near the copper wheel. The lowest temperature reached was approximately 700 K due to the high heat transfer coefficient, whose adopted value was $h_w = 1.0\ x\ 10^6 \frac{W}{m^2\ K}$.

The solidification front develops in relation to the position directions of x and y, according to the variables the process. In this situation, the inertia forces are much larger

than the viscous forces of the fluid and the thickness of the ribbon is limited of the puddle the height of the solidification front, in the end of the length of the metal puddle.

Figure 2- Temperature distribution as a function of the distance from upstream meniscus

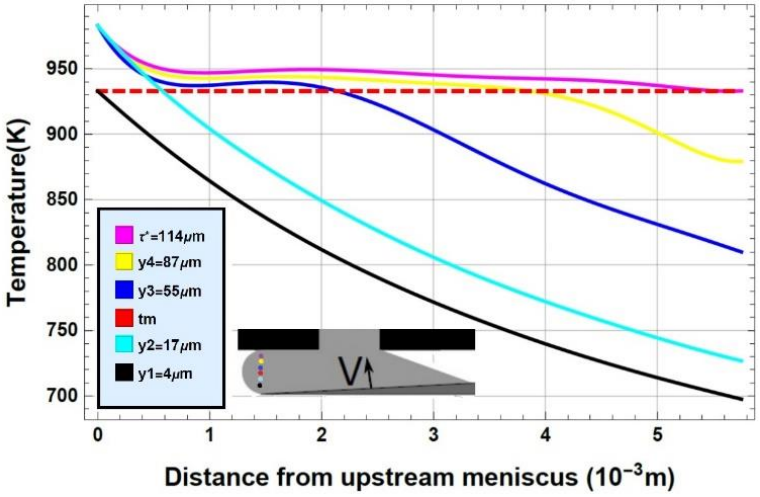

Figure 3 shows the evolution of the interface as a function of the point of start of solidification for the same metal during the process in Fig. 2, using $h_w = 5.0\ x\ 10^5 \frac{W}{m^2\ K}$. It is observed that the solidification frontier has an almost linear behavior, motivated by the short process time and the high speed of the flywheel.

Figure 3- Interface position as a function of the distance from upstream meniscus.

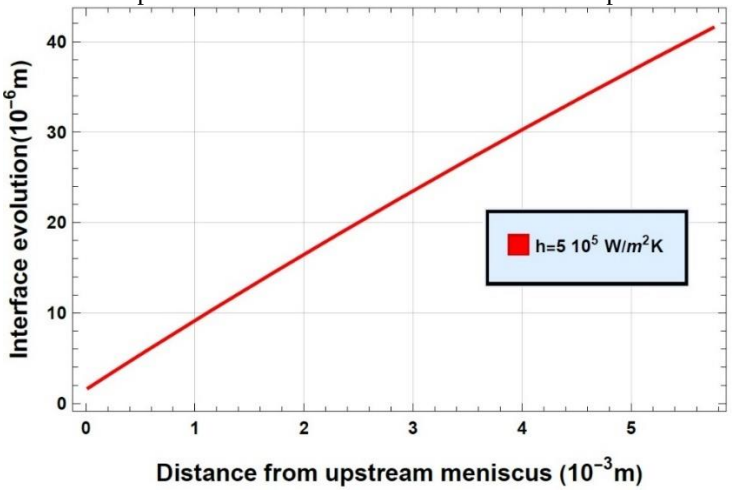

Figure 4 shows the evolution of the interface as a function of the interface velocity (m/s) varying heat transfer coefficient. As expected, the figure illustrates the fact that the interface velocity is achieved for a higher value of the heat transfer coefficient. Both the interface velocity and the interface cooling rate at high heat transfer coefficients decrease

significantly as the interface moves away from the wheel. This decrease results from the additional heat transfer resistance introduced by the growing solid layer through which the released latent heat must be conducted away. This resistance plays a proportionally greater role for large heat transfer coefficients at the wheel, which explains the faster decrease in colling rate in this case. Furthermore, we compared with the results obtained by Wang and Matthys (1992) obtaining an approximate behavior, whose difference is attributed to the model difference.

Figure 4- Interface velocity as a function of distance from the wheel for aluminum spun on wheel. Heat transfer coefficients : $2\,x\,10^5$, $5\,x\,10^5$ and $10^6\frac{W}{m^2\,K}$ $(Gap = 350\mu m$; $T_0 - T_m = 50\,K$; $ribbon\ thickness = 68\,\mu m$; $V_w = 23\frac{m}{s}$; $T_\infty = 300K$; $XD = 5.75mm$)

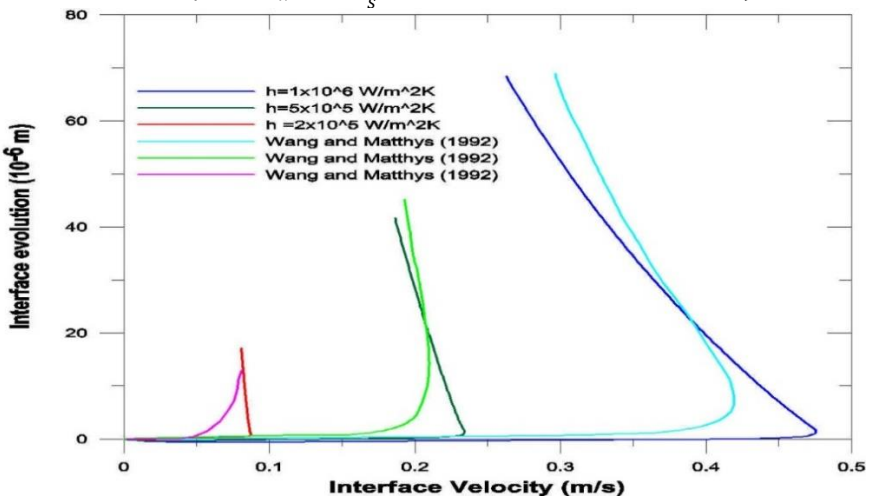

Figure 5 shows the calculated solid/liquid interface position as a function of the distance from the upstream meniscus for various puddle/wheel heat transfer coefficients when spinning aluminum on a copper wheel with the process parameters given above. These results consider the heat transfer within the wheel itself. The crucible detachment distance (X) is defined as the distance from the upstream meniscus to the point where the melt detaches from the crucible bottom surface and constitutes the downstream limit of these calculations. It can be seen in this graph that the computed thickness of the solidified layer is approximately equal to the measured final ribbon thickness (68 µm) at the detachment distance if a value of $h_w = 1.0\,x\,10^6\frac{W}{m^2\,K}$ ' is used for the heat transfer coefficient at the wheel. This implies that the ribbon would be already completely solidified within the boundaries of the puddle for this thermal contact condition. Furthermore, as we increase the heat transfer coefficient, there is an increase in the evolution of the interface, this only corroborates with physical meaning because we are

increasing the convection in the process. When comparing the solution obtained by the present work with the results obtained numerically by Wang and Matthys (1992), the curves are very close except for $h_w = 2.0\ x\ 10^6 \frac{W}{m^2\ K}$, this is probably the limit for producing tapes with a good finish.

Figure 5- Interface location as a function of the distance from the upstream meniscus for aluminum spun on a copper wheelby, varying the heat transfer coefficients: $2\ x\ 10^5$, $5\ x\ 10^5\ and\ \ 1\ \ x\ 10^6 \frac{W}{m^2\ K}$ $(Gap = 350\mu m\ \ ;\ \ T_0 - T_m = 50\ K\ \ ;\ \ thickness = 68\ \mu m\ ;\ \ \ \ V_w = 23 \frac{m}{s}\ \ ;\ T_\infty = 300K;\ \ XD = 5.75mm\ )$

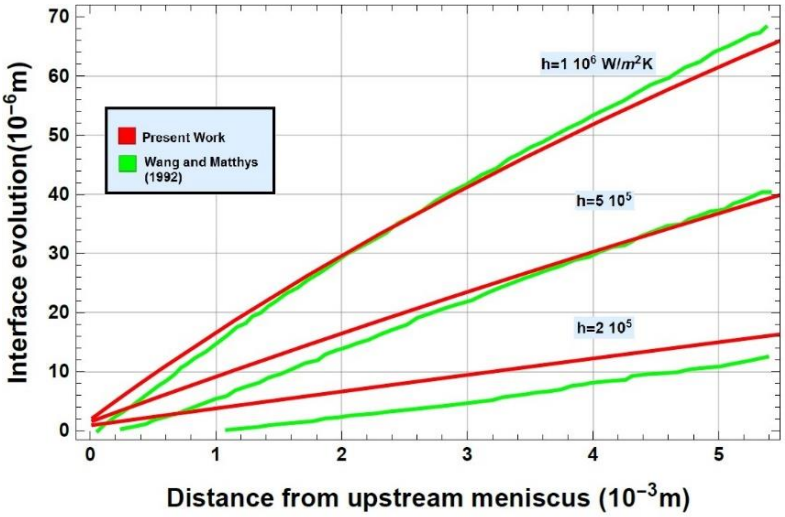

In Table 1 as we increase the number of eigenvalues, the temperature values started to converge in the fourth decimal place, this is due to the difficulty in determining the liquid / solid interface considering that the process time is very short. In addition, the height of the puddle is very small, so it is necessary to use many eigenvalues to achieve convergence.

Table 1- Convergence of the temperature of the expansion of the eigenvalues of the temperature field that refers to the distance of 114 µm from the base of the puddle, with thickness of the tape equal to 114 µm.

	Número de Autovalores						
x(mm)	**10**	**50**	**100**	**200**	**300**	**350**	**400**
0	983.000	983.000	983.000	983.000	983.000	983.000	983.000
0.575	949.013	948.978	949.031	949.129	949.215	949.256	949.296
1.150	949.004	948.977	949.034	949.137	949.228	949.272	949.314
1.725	948.595	948.582	948.646	948.762	948.866	948.915	948.963
2.300	947.678	947.669	947.742	947.874	947.991	948.047	948.102
2.875	946.256	946.236	946.314	946.459	946.588	946.650	946.711
3.450	944.362	944.324	944.402	944.550	944.685	944.750	944.814
4.025	942.030	941.988	942.059	942.197	942.326	942.389	942.451
4.600	939.304	939.285	939.341	939.453	939.560	939.612	939.665
5.175	936.257	936.271	936.304	936.370	936.435	936.468	936.500
5.750	933.000	933.000	933.000	933.000	933.000	933.000	933.000

In Table 2 shows the temperature distribution varying the distance of 21, 68 and 114 μm from the base of the puddle, in the tape with a thickness equal to 114 μm, it can be noted that as the distance from the base of the puddle decreases position of x (mm) for the 933 K temperature also decreases. In the distance of 114 μm only have liquid part because in the last position of x = 5.75 mm the temperature corresponds to 933 K, while in the distance of 21 μm have both liquid and solid part because the temperature of 933 K is in position x = 0.575 mm.

Table 2- Temperature distribution by varying the x position and y position (21 μm, 68 μm e 114 μm) for a reference ribbon thickness of 114 μm.

x(mm)	T(x,y) [K]					
	y = 21 μm		y = 68 μm		y = 114 μm	
	Present work	Nascimento (2002)	Present work	Nascimento (2002)	Present work	Nascimento (2002)
0	983.000	983.000	983.000	983.000	983.000	983.000
0.575	**933.000**	**933.000**	942.066	941.560	949.296	948.476
1.150	894.925	896.991	941.056	940.976	949.314	948.387
1.725	861.865	865.677	939.098	939.326	948.963	948.232
2.300	833.010	838.216	936.363	936.609	948.102	947.700
2.875	807.543	813.991	**933.000**	**933.000**	946.711	946.651
3.450	784.825	792.468	908.385	908.948	944.814	945.021
4.025	764.362	773.202	885.522	887.453	942.451	942.802
4.600	745.773	755.876	864.398	867.951	939.665	940.014
5.175	728.756	740.171	844.776	850.106	936.500	936.706
5.750	713.073	725.886	826.526	833.653	**933.000**	**933.000**

5 CONCLUSÃO

The Generalized Integral Transform Technique (GITT) was showing a tool capable to solve the Planar Flow Casting Problem with that can study the fast solidification of metals or alloys and obtain ribbons of thickness controlled by the speed of the wheel and for the heat transfer coefficient. Considering that the height of the puddle is very small, and the process time is very short, there is a need to use many eigenvalues to obtain the convergence of the solution.

The influence of the heat transfer coefficient at the wheel surface on the interface cooling rate and on the interface velocity was quantified. The interface velocity and interface cooling rate were seen to decrease significantly when far away from the wheel surface. It was also observed that the interface velocity shows a maximum close to the wheel surface, probaly due to the superposition of superheat and conduction resistance effects.

The interface velocity was also calculated and showed very large variations across splat cooling that are, in general, strong functions of the substrate heat transfer coefficient,

except immediately next to the substrate, where this velocity appeared to be primarily controlled by kinetics.

The results of the temperature distribution along the length of the puddle and the evolution of the solidification front were compared with results obtained Wang and Matthys (1992); Nascimento (2002) presented excellent harmony.

The solution for the representation of the Planar Flow Casting process allows the obtaining of results that can be used the engineering level. The influence of the parameters involved in the process and the relationship of these parameters with the heat transfer coefficient makes it possible to adjust the process and use different materials.

REFERÊNCIAS

Annavarapu, S., Apelian, D. and Lawley, A., "Spray casting of steel strip: process analysis". **Metallurgical Transactions A**, Vol. 21, No. 12, pp. 3237–3256,1990.

Bussmann, M., Mostaghimi, J., Kirk, D. and Graydon, J., "A numerical study of steady flow and temperature fields within a melt spinning puddle". **International journal of heat and mass transfer**, Vol. 45, No. 19, pp. 3997–4010, 2002.

Byrne, C.J., Theisen, E.A., Steen, P.H. and Reed, B.L., "Capillary puddle vibrations linked to casting-defect formation in planar-flow melt spinning". **Metallurgical and Materials Transactions B**, Vol. 37, No. 3, pp. 445–456, 2006.

Carpenter, J. and Steen, P., "Planar-flow spin-casting of molten metals: process behavior". **Journal of materials science**, Vol. 27, No. 1, pp. 215–225, 1992.

Carpenter, J. and Steen, P., "Heat transfer and solidification in planar-flow melt-spinning: high wheel speeds". **International journal of heat and mass transfer**, Vol. 40, No. 9, pp. 1993–2007, 1997.

Cotta, R.M., Integral transforms in computational heat and fluid flow. **CRC Press**, 2020.

Cox, B., "Planar-flow melt spinning: Process dynamics and defect formation", 2011.

França, R. N. C.; Miranda, G. O.; Gomes, L. G. Parâmetros térmicos, estrutura e propriedades mecânicas resultantes da solidificação horizontal das ligas de Alumínio com adição de 3 e 5% de Níquel. **Brazilian Journal of Development**, v. 6, n. 12, p. 96390-96402, 2020.

Jones, H., "The status of rapid solidification of alloys in research and application". **Journal of Materials Science**, Vol. 19, No. 4, pp. 1043–1076, 1984.

Li, D. and Lu, Z., "The effects of aging on the cyclical thermal shock response of a copper-beryllium alloy as a substrate of cooling wheel in planar flow casting process". **Materials Research Express**, Vol. 7, No. 11, p. 116511, 2020.

Li, Z., Yao, K., Li, D., Ni, X. and Lu, Z., "Core loss analysis of finemet type nanocrystalline alloy ribbon with different thickness". Progress in Natural Science: **Materials International**, Vol. 27, No. 5, pp. 588–592, 2017.

Liu, H., Chen, W., Chen, Y. and Liu, G. "Thermal deformation analysis of the rotating roller in planar flow casting process". **ISIJ international**, Vol. 50, No. 10, pp. 1431–1440, 2010.

Liu, H., Chen,W. and Liu, G., "Parametric investigation of interfacial heat transfer and behavior of the melt puddle in planar flow casting process by numerical simulation". **ISIJ international**, Vol. 49, No. 12, pp. 1895–1901, 2009a.

Liu, H., Chen,W., Qiu, S. and Liu, G., "Numerical simulation of initial development of fluid flow and heat transfer in planar flow casting process". **Metallurgical and Materials Transactions B**, Vol. 40, No. 3, pp. 411–429, 2009b.

Liu, H., Lavernia, E.J. and Rangel, R.H., "Numerical simulation of substrate impact and freezing of droplets in plasma spray processes". Journal of Physics D: Applied Physics, Vol. 26, No. 11, p. 1900, 1993.

Madireddi, S., "Effect of heat transfer between melt puddle and cooling wheel on amorphous ribbon formation". Engineering Science and Technology, an International Journal, Vol. 23, No. 5, pp. 1162–1170, 2020.

Mattson, J., Theisen, E. and Steen, P., "Rapid solidification forming of glassy and crystalline ribbons by planar flow casting". **Chemical Engineering Science**, Vol. 192, pp. 1198–1208, 2018.

Mattson, J.W., "On the production of crystalline and noncrystalline metals via the planar flow casting process", 2019.

Medeiros, M.J. and Santos, C.A.C., " Theoretical Analysis of the Rapid Solidification of Metallic Materials in Planar Flow Casting Process through of Generalized Integral Transform Technique, **26th International Congress of Mechanical Engineering**, Brazil, 2021. Miyagawa, H. K., Pontes, F.A., Curcino, I.V., Ferreira, J.R., Pontes, P.C., Macedo, E.N. and Quaresma, J.N.N et al. Integral transform of MHD flow with heat and mass transfer of a biofluid in a parallel plate channel. **Brazilian Journal of Development**, v. 5, n. 10, p. 17851-17868, 2019.

Mu, Y., Hang, L., Zhao, G., Wang, X., Zhou, Y. and Cheng, Z., "Modeling and simulation for the investigation of polymer film casting process using finite element method". **Mathematics and Computers in Simulation**, Vol. 169, pp. 88–102, 2020.

Napolitano, R.E. and Meco, H., "The role of melt pool behavior in free-jet melt spinning". **Metallurgical and Materials Transactions A**, Vol. 35, No. 5, pp. 1539–1553, 2004.

Nascimento, A.A., 2002. Theoretical Study of the Solidification of Metal Materials in Rapid Cooling using the Generalized Integral Transform Technique (in Portuguese). Ph.D. thesis, Graduate Program in Mechanical Engineering, Federal University of Paraíba, João Pessoa, Brasil, 2002.

ÖZISIK, M. N. Heat Conduction, **John Wiley & Sons**, New York, 1993.

Paz, V. F., Trevisan, L., Semeitz, A.A and Machado, E., Análise de defeitos de solidificação em componentes injetados sob pressão através da simulação numérica. **Brazilian Journal of Development**, v. 6, n. 8, p. 61077-61089, 2020.

Steen, P.H. and Karcher, C., "Fluid mechanics of spin casting of metals". **Annual review of fluid mechanics**, Vol. 29, No. 1, pp. 373–397, 1997.

Su, Y.G., Chen, F., Wu, C.Y. and Chang, M.H., "Effect of surface roughness of chill wheel on ribbon formation in the planar flow casting process". **Journal of Materials Processing Technology**, Vol. 229, pp. 609–613, 2016.

Su, Y.G., Chen, F., Wu, C.Y., Chang, M.H. and Chung, C.A., "Effects of manufacturing parameters in planar flow casting process on ribbon formation and puddle evolution of fe–si–b alloy". **ISIJ International**, Vol. 55, No. 11, pp. 2383–2390, 2015.

Swaroopa, M., Gopal, L.V., Reddy, T.K.K. and Majumdar, B., "Effect of crucible parameters on planar flow melt spinning process". **Transactions of the Indian Institute of Metals**, Vol. 68, No. 6, pp. 1125–1129, 2015.

Swaroopa, M., Reddy, T.K.K., Reddy, A.C. and Majumdar, B., "Flow cfd analysis of 2d transient melt flow from crucible on to the rotating wheel in planar melt spinning process". **Materials Today**: Proceedings, Vol. 4, No. 2, pp. 2615–2623, 2017.

Theisen, E.A. and Weinstein, S.J., . "An overview of planar flow casting of thin metallic glasses and its relation to slot coating of liquid films". **Journal of Coatings Technology and Research**, p. 1-12, 2021.

Wang, G.X. and Matthys, E., . "Modelling of rapid solidification by melt spinning: effect of heat transfer in the cooling substrate". **Materials Science and Engineering**: A, Vol. 136, pp. 85–97,1991.

Wang, G.X. and Matthys, E., "Numerical modelling of phase change and heat transfer during rapid solidification processes: use of control volume integrals with element subdivision". **International journal of heat and mass transfer**, Vol. 35, No. 1, pp. 141–153,1992.

Wang, G.X. and Prasad, V., "Rapid solidification: Fundamentals and modeling". **Annual Review of Heat Transfer**, Vol. 11, 2000.

Wang, G. and Matthys, E., "Mathematical simulation of melt flow, heat transfer and non-equilibrium solidification in planar flow casting". **Modelling and simulation in materials science and engineering**, Vol. 10, No. 1, p. 35, 2001.

Wang, T., Cai, S., Xu, J., Du, Y., Zhu, J., Xu, J. and Li, T., "Continuous casting mould for square steel billet optimised by solidification shrinkage simulation". **Ironmaking & Steelmaking**, Vol. 37, No. 5, pp. 341–346, 2010.